Geophysical Research Letters

RESEARCH LETTER
10.1029/2024GL110395

Evidence of a New Population of Weak Terrestrial Gamma-Ray Flashes Observed From Aircraft Altitude

I. Bjørge-Engeland[1], N. Østgaard[1], D. Sarria[1], M. Marisaldi[1], A. Mezentsev[1], A. Fuglestad[1], N. Lehtinen[1], J. E. Grove[2], D. Shy[2], T. Lang[3], M. Quick[3], H. Christian[4], C. Schultz[3], R. Blakeslee[3], I. Adams[5], R. Kroodsma[5], G. Heymsfield[5], K. Ullaland[1], S. Yang[1], B. Hasan Qureshi[1], J. Søndergaard[1], B. Husa[1], D. Walker[4], M. Bateman[4], D. Mach[6], P. Bitzer[4], M. Fullekrug[7], M. Cohen[8], M. Stanley[9], S. Cummer[10], J. Montanya[11], M. Pazos[12], C. Velosa[13], O. van der Velde[11], Y. Pu[10], P. Krehbiel[9], J. A. Roncancio[11], J. A. Lopez[11], M. Urbani[11], A. Santos[13], T. Neubert[14], and F. Gordillo-Vazquez[15]

[1]Department of Physics and Technology, University of Bergen, Bergen, Norway, [2]U.S. Naval Research Laboratory, Washington DC, WA, USA, [3]NASA Marshall Space Flight Center, Huntsville, AL, USA, [4]Department of Atmospheric Science, Earth System Science Center, University of Alabama, Huntsville, AL, USA, [5]NASA Goddard Space Flight Center, Greenbelt, MD, USA, [6]Universities Space Research Association, Huntsville, AL, USA, [7]University of Bath, Bath, UK, [8]Georgia Institute of Technology, Atlanta, GA, USA, [9]New Mexico Institute of Mining and Technology, Socorro, NM, USA, [10]Duke University, Durham, NC, USA, [11]Polytechnic University of Catalonia, Barcelona, Spain, [12]Instituto de Ciencias de la Atmosfera y Cambio Climatico, UNAM, CDMX, Mexico, [13]Universidad Nacional de Colombia, Medellín, Columbia, [14]Department of Space Research and Technology, Technical University of Denmark, Kongens Lyngby, Denmark, [15]Instituto de Astrofisica de Andalucia, CSIC, Granada, Spain

Key Points:

- The ALOFT flight campaign detected six TGFs within a few minutes during an ISS overpass, and none were detected by the ASIM instrument
- We show that there must be a population of TGFs that are too weak to be observed from space
- The fluence at 15 km of this population is 2–5 orders of magnitude lower than the TGFs observed from space

Supporting Information:

Supporting Information may be found in the online version of this article.

Correspondence to:

I. Bjørge-Engeland,
ingrid.engeland@uib.no

Citation:

Bjørge-Engeland, I., Østgaard, N., Sarria, D., Marisaldi, M., Mezentsev, A., Fuglestad, A., et al. (2024). Evidence of a new population of weak Terrestrial Gamma-Ray flashes observed from aircraft altitude. *Geophysical Research Letters*, *51*, e2024GL110395. https://doi.org/10.1029/2024GL110395

Received 24 MAY 2024
Accepted 11 JUL 2024

Abstract Terrestrial Gamma-ray Flashes (TGFs) are ten-to-hundreds of microsecond bursts of gamma-rays produced when electrons in strong electric fields in thunderclouds are accelerated to relativistic energies. Space instruments have observed TGFs with source photon brightness down to $\sim 10^{17}$–10^{16}. Based on space and aircraft observations, TGFs have been considered rare phenomena produced in association with very few lightning discharges. Space observations associated with lightning ground observations in the radio band have indicated that there exists a population of dimmer TGFs. Here we show observations of TGFs from aircraft altitude that were not detected by a space instrument viewing the same area. The TGFs were found through Monte Carlo modeling to be associated with 10^{15}–10^{12} photons at source, which is several orders of magnitude below what can be seen from space. Our results suggest that there exists a significant population of TGFs that are too weak to be observed from space.

Plain Language Summary Terrestrial Gamma-ray Flashes (TGFs) are short bursts of gamma-rays produced in the strong electric fields in thunderclouds. Based on space and aircraft observations, TGFs have been considered a rare phenomena. In this paper, we present observations of TGFs from an aircraft campaign that were not detected by a space instrument viewing the same area. Our results reveal that these TGFs were too weak to be observed from space, indicating a significant population of TGFs that are undetectable by space instruments.

1. Introduction

Most statistical studies on Terrestrial Gamma-ray Flashes (TGFs) are based on observations from space. Dwyer and Smith (2005) demonstrated, using Monte Carlo simulations, that for a satellite at 600 km altitude to observe TGFs produced at 15 km altitude, there would have to be an average of $\sim 10^{17}$ high-energy (>1 MeV) runaway electrons at source. Since then, Albrechtsen et al. (2018) explored whether there exists a TGF population below the lower threshold used to identify TGFs in the RHESSI data, and found that there are at least TGFs with fluence 10 times weaker than previously reported.

Since TGFs were first observed in the mid-1990s (Fishman et al., 1994), there have also been several aircraft campaigns aimed at monitoring thunderstorms and observing TGFs. Flying closer to the source one would expect to see weaker TGFs if they exist. However, the ILDAS flight campaigns (2014 and 2016), flying at up to ~12 km altitude, did not observe any TGFs (Kochkin et al., 2015, 2017), and the 2009 flight campaign ADELE, flying at 14 km altitude, detected only one TGF during 37 flight hours (Smith et al., 2011b, 2016). Based on the observations from this campaign, Smith et al. (2011a) argued that there does not exist any

significant population of TGFs weaker than those observed from space. This was supported by McTague et al. (2015), who found no new weak TGFs in a lightning-based search through Fermi data. However, this was challenged by Østgaard et al. (2012), who pointed out that based on the limited sensitivity of space instruments, one could not rule out that there exists TGFs with a source fluence down to at least 10^{12} runaway electrons at source. The existence of a population of weak TGFs was also supported by Østgaard et al. (2015) and Albrechtsen et al. (2018), who identified a population of weak TGFs in the RHESSI data. Furthermore, Abbasi et al. (2018) reported observations by ground-based detectors of downward TGFs with estimated source fluence of 10^{12}–10^{14} photons. Belz et al. (2020) argued that similar discharge processes could be involved for both downward and upward TGFs.

With the Airborne Lightning Observatory for Fly's Eye GLM Simulator and TGFs (ALOFT, GLM: Geostationary Lightning Mapper), conducted during July 2023, these earlier claims should be revised. During 10 flights and 60 flight hours total, flying at 20 km altitude, well above the thunderstorms in the Gulf of Mexico and the Caribbean, ALOFT observed >130 transient gamma-ray events.

During a flight on July 24th, the ALOFT ER-2 aircraft and the International Space Station (ISS) passed over the same geographic area during a brief time window. During this overpass, ALOFT detected six TGFs that were not detected by the Atmosphere-Space Interactions Monitor (ASIM) instrument onboard the ISS. In this paper, we present these six TGFs, and explore why they were not detected by ASIM. For three of the TGFs we have associated lightning sferic detections by the GLD360 lightning network, as well as optical measurement, giving us a reliable source location. This enables us to constrain the source fluence estimates based on Monte Carlo modeling.

2. Instruments and Data

The ER-2 aircraft containing ALOFT flew at ∼20 km altitude, whereas the ISS (containing ASIM) has an orbit at an altitude of ∼417 km.

2.1. ALOFT

ALOFT carried a suite of instruments, enabling observations of TGFs and gamma-ray glows, as well as optical and radio emissions from thunderclouds. For observing TGFs and gamma-ray glows, it contained three Bismuth-Germanate (BGO) detectors, as well as three small LYSO detectors (25, 1 and 0.09 cm^2 geometrical areas). Only detections by the BGOs will be shown here. The BGOs had the capability to detect gamma-rays with energies 300 keV-40 MeV, and each BGO had a size of $15 \times 5 \times 3.2$ cm^3. The three BGOs have a total geometric area of 225 cm^2. The maximum effective area is ∼160 cm^2 for events at 0° nadir angle, assuming a standard RREA spectrum from a source at 15 km altitude. Based on modeling (Hansen et al., 2013) the BGOs should be able to detect TGFs out to ∼20 km from the ALOFT footpoint, given a source fluence of 10^{17}. In addition to BGO and LYSO detectors, ALOFT was equipped with the in-Situ Thunderstorm Observer for Radiation Mechanism (iSTORM), which is a spectrometer covering an energy range from ∼300 keV to >5 MeV and has a geometric area of 157 cm^2 (Marisaldi et al., 2024; Østgaard et al., 2024). The BGO and iSTORM data acquisition systems were completely independent.

For detecting optical emissions from lightning, ALOFT was equipped with a Fly's Eye GLM Simulator (FEGS), which is an array of multi-spectral radiometers (Quick et al., 2020). FEGS contains 30 radiometers, observing emissions in a range of wavelengths, with a temporal resolution of 10 μs and a field-of-view (FOV) extending up to ∼5–10 km from the footpoint, depending on the cloud top height (Quick et al., 2020). FEGS contains a 5×5 grid of radiometers for observing emissions at 777.4 nm (corresponding to emissions from hot lightning leaders) with each radiometer being tilted at different angles, combining to form an image of the cloud top (Chanrion et al., 2019; Quick et al., 2020). Each radiometer has a square FOV with 9.46° viewing angle, and they are separated by 18° in the x- and *y*-direction. FEGS also includes a radiometer for observing emissions at 337 nm (corresponding mainly to streamer emissions), oriented to view in nadir direction. For the events discussed in this paper the cloud top was at 17 km, giving an approximate −3 to +3 km "square" FOV for FEGS. ALOFT also included electric field change meters, microwave radiometers and radar systems.

Table 1
Properties of the Six TGFs

TGF	Time [UTC]	Lat	Lon	d_{ISS} [km]	T_{core90} [μs]	BGO counts	ALOFT$_{area}$ [cm^2]	Cnts/cm^2	d_{GLD} [km]	d_{FEGS}	PC [kA]	ASIM$_{area}$ [cm^2]
1	06:44:09.774	19.1899	−93.7270	329[b]	280	134	95	1.41	12.5	-	32	126
2	06:45:27.586	19.0964	−93.6179	212[a]	70	64	153	0.42	-	3 ± 3	-	159
3	06:45:28.422	19.0954	−93.6167	218[a]	180	102	157	0.65	-	1 ± 1	-	158
4	06:45:38.618	19.0832	−93.6028	288[b]	50	68	128	0.53	3.0	-	5	168
5	06:45:39.205	19.0825	−93.6020	292[a]	60	87	153	0.57	-	3 ± 3	-	169
6	06:45:48.174	19.0717	−93.5897	354[b]	30	72	144	0.50	5.2	-	7	172

[a]d_{ISS} represents the distance between the ISS and the ALOFT location. [b]d_{ISS} represents the distance between the ISS and the sferic location.

2.2. ASIM

The ASIM payload has been mounted on the Columbus module of the ISS since April 2018, and consists of the two instruments Modular X- and Gamma-ray Sensor (MXGS) (Østgaard, Balling, et al., 2019) and the Modular Multi-spectral Imaging Array (MMIA) (Chanrion et al., 2019). MXGS detects TGFs and MMIA observes optical signals from lightning and Transient Luminous Events (TLEs). MXGS consists of a High-Energy Detector (HED) and a Low-Energy Detector (LED). The HED contains 12 BGOs (identical to those on ALOFT), each coupled to a photomultiplier tube (PMT), and detects gamma-rays in the energy range 300 keV to >30 MeV. ASIM was initially mounted on the lower deck of the Columbus module facing nadir, with an effective area of ∼650 cm^2 at 1 MeV. ASIM was since re-positioned (January 2022), with the MMIA instruments facing toward the limb. With the new configuration, the maximum effective area of MXGS is reduced by a factor of ∼5 for events at 0° nadir. The effective area for both ALOFT and ASIM for each of the events discussed in this paper are given in Table 1 (columns 8 and 13).

The MXGS and MMIA instruments can both trigger individually and cross-trigger (Østgaard, Neubert, et al., 2019). When one instrument is triggered, 2 seconds of data are captured, and a cross-trigger is sent to the other instrument. MXGS triggers when the number of counts detected within a specific time window exceeds a threshold value (representing a background value). As outlined in Østgaard, Balling, et al. (2019), MXGS operates with three short trigger windows (300 µs, 1 and 3 ms) and one long trigger window (25 ms).

2.3. GLD360

For getting an accurate source location for the TGFs detected by ALOFT during the ISS overpass, we used data from the global ground-based lightning location network GLD360. The network uses sensors in the 500 Hz-50 kHz range, and employs a time of arrival technique, as well as magnetic direction finding for geo-locating strokes (Said & Murphy, 2016). GLD360's median location accuracy is ∼2 km, and an uncertainty ellipse is provided for each stroke location (Rudlosky et al., 2017; Said & Murphy, 2016).

3. Observations

Within less than 2 min following 06:44 UTC on the 24th of July, ALOFT detected six TGFs within 360 km from the ISS footpoint (exact values are given in Table 1). The distances between the ISS footpoint and the ALOFT location at the time of TGF detection are shown in Figure 1. The first event was detected in front of the ISS, whereas the other five were detected behind the ISS. The counts detected by the BGOs and iSTORM for TGFs 1–6 are presented in panels a–f in Figure 2 and in Table 1. For TGF 6, iSTORM was in a periodic, system-induced dead interval. The TGFs had T_{core90} durations between 30 and 280 µs, and between 64 and 134 counts were detected by the BGOs for the TGFs. The T_{core90} duration (the shortest interval including 90% of the counts) was determined by using a similar approach as Lindanger et al. (2021), Bjørge-Engeland et al. (2022) and Skeie et al. (2022).

3.1. GLD Associations and FEGS Signals

GLD360 detected sferics (radio emissions from lightning discharges) close in time and location to TGFs 1, 4 and 6. The radial distance between the GLD detections and ALOFT, as well as the peak currents reported by GLD360 are listed in Table 1.

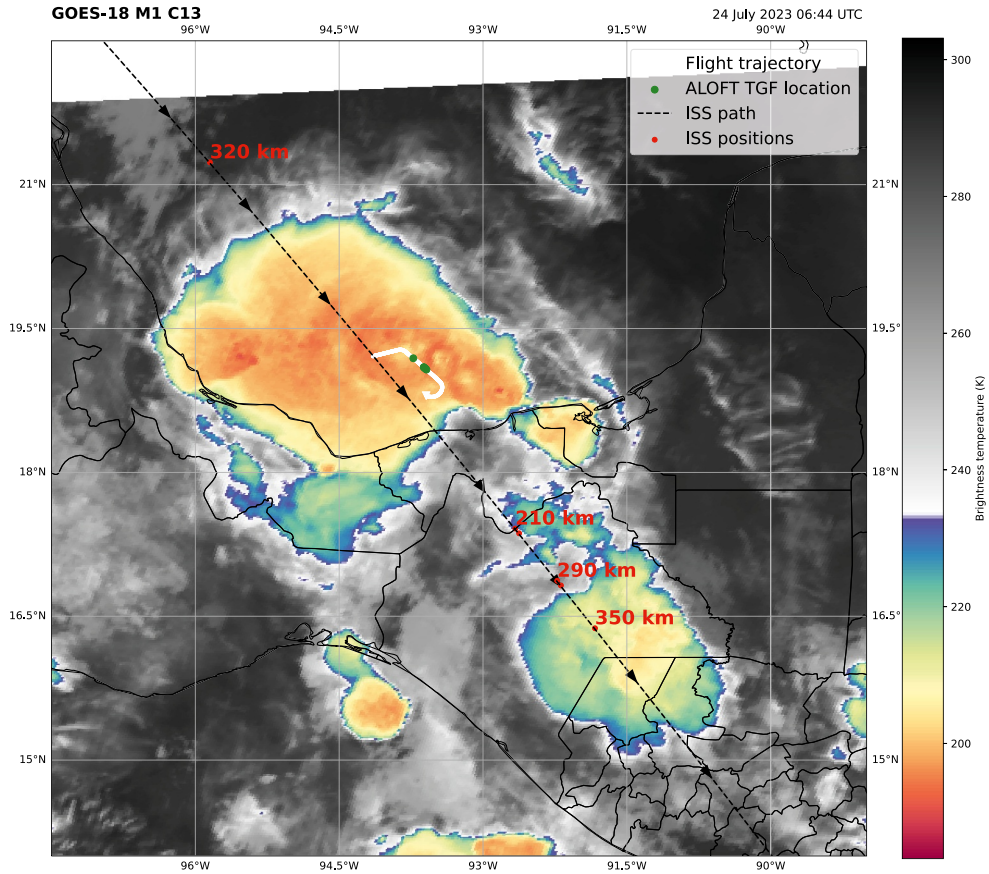

Figure 1. Map of the ALOFT detections (green markers) with respect to the ISS path, using an image from the Advanced Baseline Imager instrument, channel 13 (longwave IR), onboard the GOES-18 satellite (at 06:44 UTC) of the brightness temperature of the cloud system. The white path marks the aircraft trajectory from 06:40 to 06:50 UTC. Red markers highlight the distance between the ISS path and ALOFT locations at the time of TGF detections (exact values given in Table 1).

Panels g–l in Figure 2 show the FOVs of the FEGS photometers projected onto the cloud top, found to be at 17 km from ALOFT radar data, for each of the six TGFs. In panels *g*, *j* and *l*, the blue marker denotes the location of the lightning stroke detected by GLD360, while the ellipse represents the uncertainty of this location. The brightest part of the grid indicates the strongest incoming signal. Only the first TGF had a source location clearly outside the FEGS FOV, with a GLD360 location at 12.5 km radial distance and no clear optical signals were detected. However, considering the uncertainty ellipse, the actual location of the GLD could be 11–15 km from the footpoint.

The radial distance between the sferic association to TGF 4 and the ER-2 footpoint was just 3 km, and most FEGS photometers detected strong signals. For TGF 6, only a few photometers detected strong signals. As shown in Figure 2l, the projected photometer FOVs right of the aircraft are brighter than those closer to the source location detected by GLD360. Since the sferic detection fits well with respect to both time and location relative to ALOFT, this could be attributed to scattering within the cloud and different parts of the cloud being illuminated. There were no associated GLD locations for TGFs 2, 3 and 5, but the distance between the source and the ER-2 footpoint can be estimated from FEGS images. For TGF 3, the location from FEGS images is ∼1 ± 1 km. For TGFs 2 and 5 the location appears to be at the edge of the FEGS FOV (∼3 km from the footpoint). Assuming the optical signal from a source within the cloud would scatter to cover ±3 km at the cloud top, these TGFs have a source 3 ± 3 km from the aircraft. All the distances from the aircraft footpoint to GLD and FEGS locations are given in Table 1.

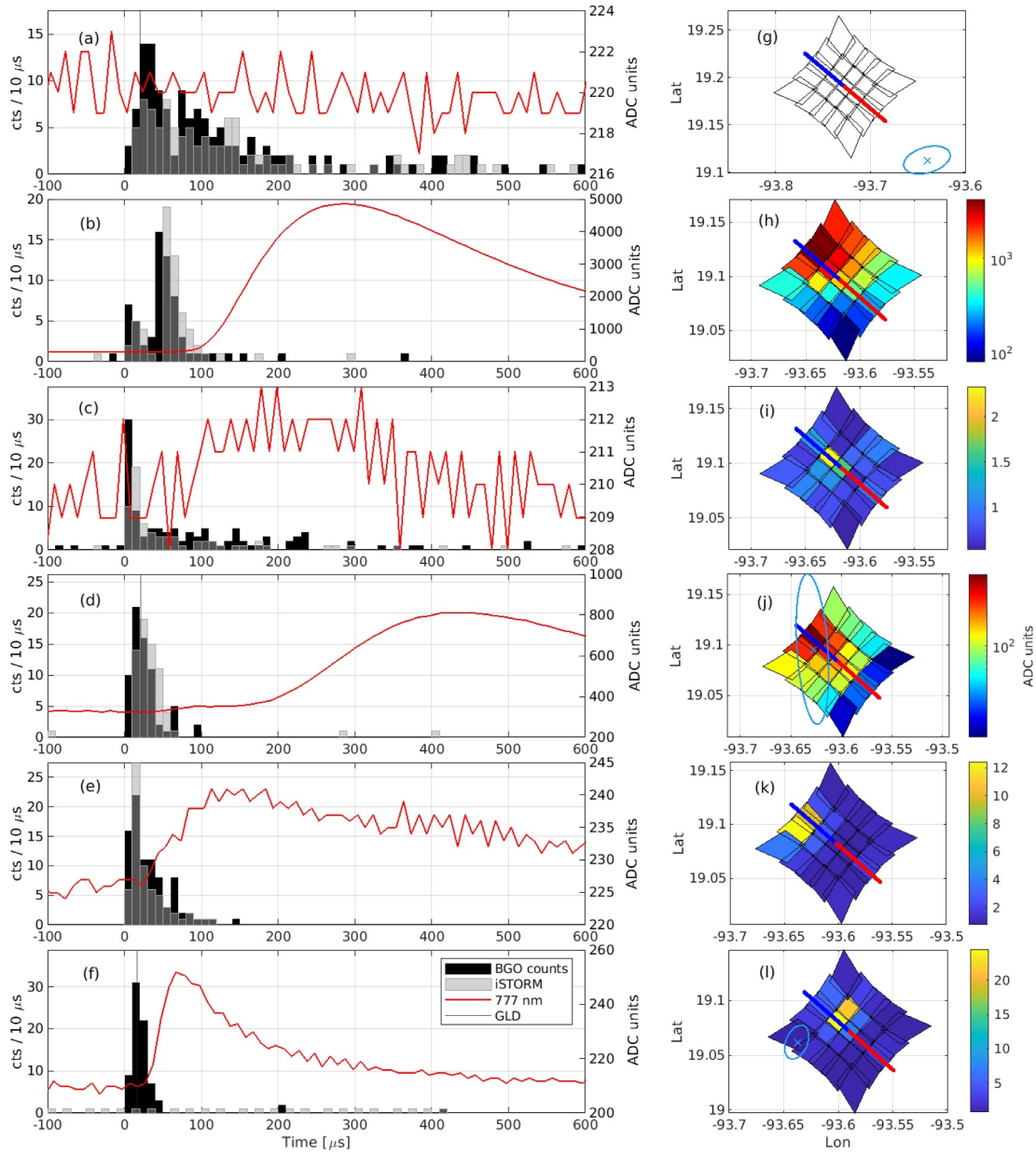

Figure 2. TGFs detected by ALOFT BGOs during the ISS overpass. Panels a–f show counts detected by ALOFT BGOs and iSTORM for TGFs 1–6 (Table 1), as well as the maximum 777 nm signal detected by FEGS, with zero on the *x*-axis representing the onset of the TGF detection by ALOFT BGOs. Panels g–l show projections of FEGS observations onto the cloud top for TGFs 1–6. The aircraft is moving from left to right. Each box in the grid represents the FOV of one of the 777 nm photometers. The brightest boxes represent the photometers detecting the strongest signals. Notice that the colorscales used in panels g–l for the optical brightness differ by up to two orders of magnitude (ADC units with background subtracted). For TGF 1, no clear signals were detected by any photometers. The blue crosses in panels g (TGF 1), j (TGF 4) and l (TGF 6) represent the GLD location of the lightning stroke, and blue ellipses represent the uncertainty in these locations.

3.2. Observations by ASIM

ASIM triggered 46 times between 06:42 and 06:46 UTC on July 24th between latitudes 26° and 15°. Nearly all these triggers were MMIA triggers. With MMIA viewing toward the limb, the lightning strokes that triggered MMIA were far away from the ALOFT FOV. Coincidentally, one of the ALOFT TGFs (TGF 2 in Table 1) was detected within the time interval covered by an MMIA trigger. As outlined in Section 2.2, if MXGS coincidentally detected a TGF during the 2 s of data already being captured due to the MMIA trigger, MXGS itself would not trigger again on the event. There was an increase in the number of counts detected by the MXGS BGOs within [-40, 40] ms (taking into account the absolute timing uncertainty of ASIM) around the ALOFT detection time for

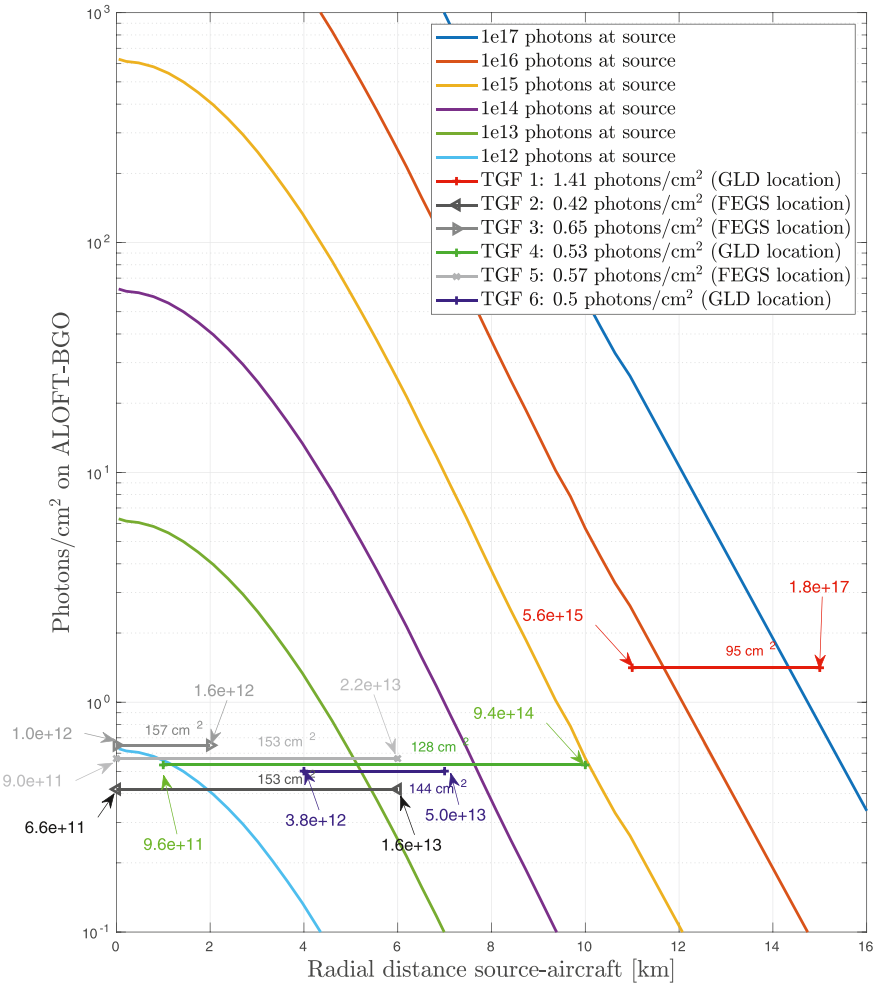

Figure 3. Modeled fluence on ALOFT BGOs for sources at radial distances indicated by the *x*-axis for different numbers of photons at source (at 15 km), at observation altitude 20 km. We assume a vertical and upward TGF with a RREA spectrum and a Gaussian 30° angular distribution. Source energy minimum and maximum thresholds were 100 keV and 40 MeV, respectively, and the recorded energy minimum and maximum thresholds were 300 keV and 40 MeV. The horizontal lines correspond to the fluence on ALOFT BGOs and the text displayed above indicates the ALOFT BGO effective areas for the events. The arrows indicate the minimum and maximum source photon brightness. The extent of the horizontal lines corresponds to the uncertainty in the distance from the ALOFT footpoint to the GLD location for TGFs 1, 4 and 6 (see uncertainty ellipses in Figure 2, panels g, j and l) and the uncertainty in the location given by FEGS detections for TGFs 2, 3 and 5.

TGF 2, which was also prominent when using a sliding window corresponding to the MXGS trigger windows (Figure S1 in Supporting Information S1). However, the counts causing a peak in the detected number of counts occurred within 1 μs of each other, implying that they originated from incoming cosmic particles rather than the event below ALOFT (Figure S2 in Supporting Information S1). For these types of events MXGS also would not trigger.

4. Discussion

To explore why the six TGFs were not observed by ASIM, we used a Monte Carlo model to find the number of photons at source corresponding to the observed fluence on the ALOFT BGOs. We used 15 km as a reference source altitude, a Gaussian angular distribution of 30°, and a RREA spectrum to estimate expected fluence (counts/cm^2) at 20 km as a function of radial distance from source with fluences 10^{17}–10^{12}, shown in Figure 3. Knowing the source location (determined from FEGS and GLD360), we calculated the

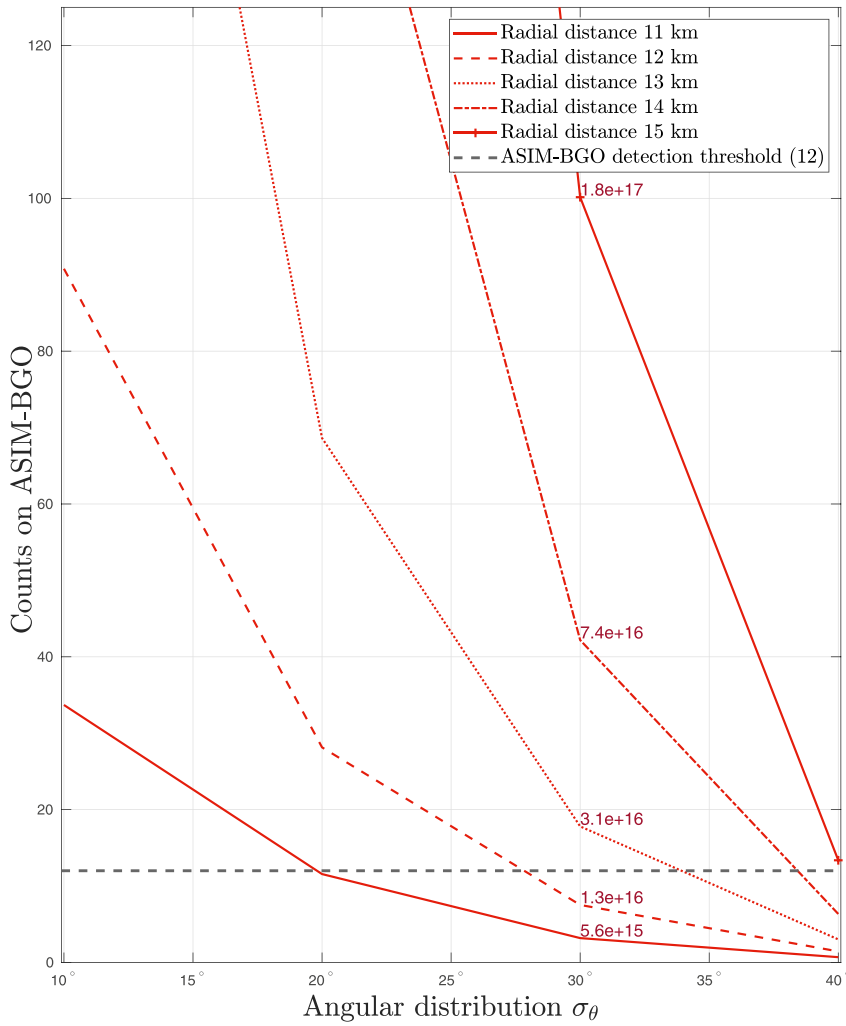

Figure 4. Modeled number of counts on the ASIM BGOs for a source at radial distances 11–15 km from ALOFT, for different angular distributions. The horizontal line represents the detection threshold for ASIM. The values displayed next to each red line correspond to the source photon brightness at that source-aircraft radial distance for an angular distribution of 30°, assuming a point source.

effective detection area for each event (Table 1), and got the measured fluence as counts/cm^2, shown for all six events as horizontal lines in Figure 3. The extent of the horizontal lines corresponds to the possible aircraft-source distances, given by the uncertainty in the GLD360 and FEGS-determined locations. For TGFs 2–6, the source fluence is between ~6.6×10^{11} and 10^{15}, which is 2–5 orders of magnitude lower than what can be detected from space, if we assume 10^{17} photons at 15 km to be the required brightness to be observed from space. As Dwyer and Smith (2005) found that there must be on average ~10^{17} runaway electrons at a source of 15 km for the TGF to be observed by RHESSI at 600 km altitude, and ASIM has a larger effective area (before repositioning to the limb viewing position), we would expect ASIM to be able to observe TGFs with a source photon brightness of ~10^{16}. However, with the current configuration of MXGS, the effective area is significantly reduced in the nadir direction. The fluence and source-aircraft radial distance for TGF 1 correspond to the largest number of photons at source (5.6×10^{15}–1.8×10^{17}), indicating that this TGF could have been seen from space.

To investigate the non-detection by ASIM of TGF 1 further, we present in Figure 4 the expected number of counts on ASIM BGOs considering different angular distributions (Gaussian σ 10°–40°) and radial distances (based on the uncertainty ellipse for the GLD location). For TGF 1, the effective areas of the ASIM and ALOFT BGOs were 126 and 95 cm^2, respectively. The gray horizontal line represents the threshold number of counts required on the

ASIM BGO detectors for MXGS to trigger in the 300 μs trigger window, given the background level. The red lines below the threshold indicate which angular distributions and radial distances could explain the non-detection of TGF 1. The numbers displayed next to the red lines correspond to the model-estimated source photon brightness corresponding to that radial distance. Figure 4 shows that the non-detection is consistent with a Gaussian 20°–30° angular distribution, which is also the realistic angular distribution interval from scattering of electrons and photons in the atmosphere. This means that the source location for TGF 1 was most likely 11–12 km from the ER-2 footpoint. If the source was 14 km away, with an angular distribution of 30°, ASIM BGOs should have detected >40 counts and MXGS would have triggered on the event. Similarly, if the source was 15 km away, ASIM should have detected this TGF. Since ASIM did not trigger, a source distance of 11–12 km is more likely, and the source photon brightness for TGF 1 is $\sim 10^{16}$. This is the only TGF for which an ASIM detection could have been possible.

The non-detection by ASIM of the six TGFs during the ISS overpass indicates that there is a population of TGFs that are too weak to be observed from space, with a source photon brightness 2–5 orders of magnitude (10^{15}–10^{12}) lower than what is usually attributed to TGF observations from space. This may indicate that a higher percentage of lightning than previously thought are associated with TGFs. Using data from RHESSI, Smith et al. (2016) suggested that <1% of lightning detected by the World Wide Lightning Location Network (WWLLN) are associated with a TGF, and that there is only a small population of TGFs within 10^{-4} of RHESSI's detection threshold. Although our sample of events is limited in size, all of our events, with the exception of TGF 1, are several orders of magnitude below RHESSI's detection threshold, suggesting that there very likely is a larger population of TGFs that are several orders of magnitude too weak to be observed from space. This supports the conclusions of Østgaard et al. (2012); Gjesteland et al. (2012); Hansen et al. (2013); Abbasi et al. (2018) and Albrechtsen et al. (2018).

5. Conclusion

From the non-detection by ASIM of TGFs observed by ALOFT during the ISS overpass we can conclude the following.

- All but one of the TGFs observed by ALOFT during the overpass were far too weak to be observed from space
- For the TGF with the largest fluence (TGF 1), the non-detection by ASIM can likely be explained by a 30° Gaussian angular distribution, for a source 11–12 km from the ER-2 footpoint
- Modeling results show that the source photon brightness for TGFs detected by ALOFT can be 2–5 orders of magnitude (10^{15}–10^{12}) lower than that for TGFs observed from space
- Our results suggest that there exists a large population of TGFs that cannot be observed from space

Data Availability Statement

The data used in this study are available on Zenodo: https://doi.org/10.5281/zenodo.12636189 (Bjørge-Engeland, 2024).

Acknowledgments
This work made use of data from UIB-BGO, iSTORM, FEGS, EFCM, LF and VHF, GLD360. The ALOFT campaign and the UIB-BGO instrument were supported by European Research Council under the European Union's Seventh Framework Programme (FP7/2007–2013)/ERC grant agreement no. 320839 and the Research Council of Norway under contracts 223252/F50 (CoE) and contract 325582. Work at NRL on ALOFT is supported by the Office of Naval Research 6.1 funds. In addition, D. Shy is supported by the U.S. Naval Research Laboratory's Jerome and Isabella Karle Fellowship. The FEGS and EFCM team acknowledge the work of Scott Podgorny, David Corredor, and Mike Stewart. S. Cummer and Y. Pu were partly supported by the National Science Foundation Dynamic and Physical Meteorology program through Grant AGS-2026304. The participation of J.A.R, J.L., M.U., O.vdV. and J.M. and the fielding of instruments on San Andrés island was supported by projects EQC2021-006957-P and PID2022-136348NB-C33 by the government of Spain (MCIN/AEI/10.13039/501100011033) and the European Regional Development Fund "ERDF - A way of making Europe" by the European Union. The use of the VHF data was supported by US NSF Grants 1720600 and 2214044. M.F. was sponsored by the Royal Society (UK) grant NMG/R1/180252 and the Natural Environment Research Council (UK) under grants NE/L012669/1 and NE/H024921/1. Significant financial and logistical support for ALOFT was provided by the NASA Earth Science Division. We thank the governments of Mexico, Bahamas, Colombia, Belize, Guatemala, Honduras, Nicaragua, Panama, Dominican Republic, Costa Rica, El Salvador, Haiti, Turks and Caicos, Jamaica, and the Cayman Islands for approving ER-2 overflights in support of ALOFT. GOES MDS sectors in support of ALOFT were enabled by NOAA. We want to thank the ER-2 Project Team at NASA Armstrong Flight Research Center, and the MacDill Air Force Base for hosting. The simulations were performed on resources provided by UNINETT Sigma2 - the National Infrastructure for High Performance Computing and Data Storage in Norway, under project no. NN9526 K. Francisco J. Gordillo-Vázquez was supported by project PID2022-136348NB-C31 funded by MCIN/AEI. The authors wish to thank VAISALA for the GLD360 lightning data.

References

Abbasi, R. U., Abu-Zayyad, T., Allen, M., Barcikowski, E., Belz, J. W., Bergman, D. R., et al. (2018). Gamma ray showers observed at ground level in coincidence with downward lightning leaders. *Journal of Geophysical Research: Atmospheres*, *123*(13), 6864–6879. https://doi.org/10.1029/2017JD027931

Albrechtsen, K. H., Østgaard, N., Berge, N., & Gjesteland, T. (2018). Observationally weak TGFs in the RHESSI data. *Journal of Geophysical Research: Atmospheres*, *124*(1), 287–298. https://doi.org/10.1029/2018JD029272

Belz, J. W., Krehbiel, P. R., Remington, J., Stanley, M. A., Abbasi, R. U., LeVon, R., et al. (2020). Observations of the origin of downward terrestrial gamma-ray flashes. *Journal of Geophysical Research: Atmospheres*, *125*(23). https://doi.org/10.1029/2019JD031940

Bjørge-Engeland, I. (2024). Supporting information for the paper "Evidence of a new population of weak Terrestrial Gamma-ray Flashes observed from aircraft altitude" by Bjørge-Engeland et al. [Dataset]. https://doi.org/10.5281/zenodo.12636189. *Zenodo*

Bjørge-Engeland, I., Østgaard, N., Mezentsev, A., Skeie, C. A., Sarria, D., Lapierre, J., et al. (2022). Terrestrial gamma-ray flashes with accompanying elves detected by ASIM. *Journal of Geophysical Research: Atmospheres*, *127*(11), 1–21. https://doi.org/10.1029/2021JD036368

Chanrion, O., Neubert, T., Lundgaard Rasmussen, I., Stoltze, C., Tcherniak, D., Jessen, N. C., et al. (2019). The modular multispectral imaging array (MMIA) of the ASIM payload on the international space station. *Space Science Reviews*, *215*(4), 28. Retrieved from https://doi.org/10.1007/s11214-019-0593-y

Dwyer, J. R., & Smith, D. M. (2005). A comparison between Monte Carlo simulations of runaway breakdown and terrestrial gamma-ray flash observations. *Geophysical Research Letters*, *32*(22), 1–4. https://doi.org/10.1029/2005GL023848

Fishman, G. J., Bhat, P. N., Mallozzi, R., Horack, J. M., Koshut, T., Kouveliotou, C., et al. (1994). Discovery of intense gamma-ray flashes of atmospheric origin. *Technical Reports Series*, *264*(5163), 1313–1316. https://doi.org/10.1126/science.264.5163.1313

Gjesteland, T., Østgaard, N., Collier, A. B., Carlson, B. E., Eyles, C., & Smith, D. M. (2012). A new method reveals more TGFs in the RHESSI data. *Geophysical Research Letters*, *39*(5), 1–5. https://doi.org/10.1029/2012GL050899

Hansen, R. S., Østgaard, N., Gjesteland, T., & Carlson, B. (2013). How simulated fluence of photons from terrestrial gamma ray flashes at aircraft and balloon altitudes depends on initial parameters. *Journal of Geophysical Research: Space Physics*, *118*(5), 2333–2339. https://doi.org/10.1002/jgra.50143

Kochkin, P., Van Deursen, A. P., De Boer, A., Bardet, M., & Boissin, J. F. (2015). In-flight measurements of energetic radiation from lightning and thunderclouds. *Journal of Physics D: Applied Physics*, *48*(42), 425202. https://doi.org/10.1088/0022-3727/48/42/425202

Kochkin, P., van Deursen, A. P., Marisaldi, M., Ursi, A., de Boer, A. I., Bardet, M., et al. (2017). In-flight observation of Gamma ray glows by ILDAS. *Journal of Geophysical Research: Atmospheres*, *122*(23), 801–812. https://doi.org/10.1002/2017JD027405

Lindanger, A., Marisaldi, M., Sarria, D., Østgaard, N., Lehtinen, N., Skeie, C. A., et al. (2021). Spectral analysis of individual terrestrial gamma-ray flashes detected by ASIM. *Journal of Geophysical Research: Atmospheres*, *126*(23), 1–18. https://doi.org/10.1029/2021jd035347

Marisaldi, M., Østgaard, N., Mezentsev, A., Lang, T., Grove, J. E., Shy, D., et al. (2024). Highly dynamic gamma-ray emissions are common in tropical thunderclouds. *Nature*. (accepted). https://doi.org/10.1038/s41586-024-07936-6

McTague, L. E., Cummer, S. A., Briggs, M. S., Connaughton, V., Stanbro, M., & Fitzpatrick, G. (2015). A lightning-based search for nearby observationally dim terrestrial gamma ray flashes. *Journal of Geophysical Research*, *120*(23), 003–012. https://doi.org/10.1002/2015JD023475

Østgaard, N., Albrecthsen, K. H., Gjesteland, T., & Collier, A. (2015). A new population of terrestrial gamma-ray flashes in the RHESSI data. *Geophysical Research Letters*, *42*(24), 10937–10942. https://doi.org/10.1002/2015GL067064

Østgaard, N., Balling, J. E., Bjørnsen, T., Brauer, P., Budtz-Jørgensen, C., Bujwan, W., et al. (2019a). The modular X- and gamma-ray sensor (MXGS) of the ASIM payload on the international space station. *Space Science Reviews*, *215*(2), 23. https://doi.org/10.1007/s11214-018-0573-7

Østgaard, N., Gjesteland, T., Hansen, R. S., Collier, A. B., & Carlson, B. (2012). The true fluence distribution of terrestrial gamma flashes at satellite altitude. *Journal of Geophysical Research*, *117*(3). https://doi.org/10.1029/2011JA017365

Østgaard, N., Mezentsev, A., Marisaldi, M., Grove, J. E., Quick, M., Christian, H., et al. (2024). Flickering gamma-ray flashes, the missing link between gamma glows and TGFs. *Nature*. (accepted). https://doi.org/10.1038/s41586-024-07893-0

Østgaard, N., Neubert, T., Reglero, V., Ullaland, K., Yang, S., Genov, G., et al. (2019b). First 10 Months of TGF observations by ASIM. *Journal of Geophysical Research: Atmospheres*, *124*(24), 14024–14036. https://doi.org/10.1029/2019JD031214

Quick, M. G., Christian, H. J., Virts, K. S., & Blakeslee, R. J. (2020). Airborne radiometric validation of the geostationary lightning mapper using the Fly's Eye GLM Simulator. *Journal of Applied Remote Sensing*, *14*(04). https://doi.org/10.1117/1.jrs.14.044518

Rudlosky, S. D., Peterson, M. J., & Kahn, D. T. (2017). GLD360 performance relative to TRMM LIS. *Journal of Atmospheric and Oceanic Technology*, *34*(6), 1307–1322. https://doi.org/10.1175/JTECH-D-16-0243.1

Said, R. K., & Murphy, M. J. (2016). GLD360 upgrade: Performance analysis and applications. *24th International Lightning Detection Conference(Ic)*.

Skeie, C. A., Østgaard, N., Mezentsev, A., Bjørge-Engeland, I., Marisaldi, M., Lehtinen, N., et al. (2022). The temporal relationship between terrestrial gamma-ray flashes and associated optical pulses from lightning. *Journal of Geophysical Research: Atmospheres*, *127*(17), 1–14. https://doi.org/10.1029/2022JD037128

Smith, D. M., Buzbee, P., Kelley, N. A., Infanger, A., Holzworth, R. H., & Dwyer, J. R. (2016). The rarity of terrestrial gamma-ray flashes: 2. RHESSI stacking analysis. *Journal of Geophysical Research*, *121*(19), 11382–11404. https://doi.org/10.1002/2016JD025395

Smith, D. M., Dwyer, J. R., Hazelton, B. J., Grefenstette, B. W., Martinez-Mckinney, G. F., Zhang, Z. Y., et al. (2011b). A terrestrial gamma ray flash observed from an aircraft. *Journal of Geophysical Research*, *116*(20), 1–10. https://doi.org/10.1029/2011JD016252

Smith, D. M., Dwyer, J. R., Hazelton, B. J., Grefenstette, B. W., Martinez-Mckinney, G. F., Zhang, Z. Y., et al. (2011a). The rarity of terrestrial gamma-ray flashes. *Geophysical Research Letters*, *38*(8). https://doi.org/10.1029/2011GL046875